

we live in a universe that is geometrically flat, with a fractional contribution of the total mass over the critical mass (required for a flat universe) of $\Omega_{\text{matter}} h^2 \approx 0.2$, where the reduced Hubble constant is $h = H_0/100 \text{ km s}^{-1} \text{ Mpc}^{-1}$. The remaining contribution to the critical mass must come in some form of dark energy (specified as Ω_{vacuum}). The CMB data also indicate the detection of the second acoustic peak that, along with the first peak, can constrain the density of baryons in the universe (Ω_{baryons}).

Until recently, the use of the local matter distribution in the universe has been limited to constraining just $\Omega_{\text{matter}} h$ because the data sets were not large enough to detect the acoustic oscillations. On scales smaller than $\sim 50h^{-1}$ Mpc, the oscillations will be wiped out by the individual motions of galaxies and clusters. Here, we examine the matter-density power spectrum on near-gigaparsec scales, where the imprint of the acoustic oscillations should be detectable. For our study, we use clusters of galaxies and individual galaxies as tracers of the matter in the universe and describe their distribution by the power spectrum, $P(k)$, of fluctuations in this density field, $\delta(\mathbf{r})$:

$$\delta(\mathbf{r}) = \frac{\rho(\mathbf{r}) - \langle \rho \rangle}{\langle \rho \rangle} \quad (1)$$

The power spectrum is a function of wave number $k = 2\pi/\lambda$, where λ is the scale size in units of h^{-1} Mpc. We derived $P(k)$ from three cosmological redshift surveys: the Abell/ACO Cluster Survey (9, 10), the IRAS Point Source redshift catalog (PSCz) (11, 12), and the Automated Plate Measuring Machine (APM) cluster catalog (13, 14). The volumes traced by these surveys are large enough to accurately probe the power spectrum to near-gigaparsec scales.

We find oscillatory features in the matter-density power spectrum (Fig. 1B), consistent with a cosmological model having $\Omega_{\text{matter}} h^2 = 0.12_{-0.03}^{+0.02}$, $\Omega_{\text{baryons}} h^2 = 0.029_{-0.015}^{+0.011}$, and $n_s = 1.08_{-0.20}^{+0.17}$ where n_s is the primordial spectra index (2σ confidence limits) (15, 16). These fitted parameters provide almost enough information to independently predict the CMB temperature spectrum free of any CMB data. All that is needed is a choice for Ω_{vacuum} , which affects the temperature power spectrum but has no effect on the shape of the local matter-density power spectrum (17). Fortunately, the recent Type Ia supernovae results provide us with an independent measurement of Ω_{vacuum} (18, 19). Thus, using the data at redshift ≈ 0.1 from galaxies and clusters of galaxies, along with the recent supernovae data at redshift ≈ 1 , we can accurately predict the CMB temperature power spectrum (Fig. 1A) at redshift ≈ 1000 , under the assumption of the standard cosmological model.

We see a direct concordance between the CMB, which originated $\approx 100,000$ years after the Big Bang, the supernovae data, measured

at roughly half the age of the universe, and the matter-density distribution, which is measured today. Not only do these results provide support for the Hot Big Bang Inflationary model, they also show that we understand the physics of the early universe. This physics can take us forward in time, predicting the matter-density distribution from the CMB, or, as we have shown here, backward in time, "predicting" the CMB using the distribution of galaxies and clusters in our local universe.

References and Notes

1. P. J. E. Peebles, *Principles of Physics Cosmology* (Princeton Univ. Press, NJ, 1993).
2. ———, J. T. Yu, *Astrophys. J.* **162**, 815 (1970).
3. W. Hu, M. White, *Astrophys. J.* **471**, 30 (1996).
4. A. D. Miller *et al.*, *Astrophys. J.* **524L**, 1 (1999).
5. A. Balbi *et al.*, *Astrophys. J.* **545**, L1 (2000).
6. A. Melchiorri *et al.*, *Astrophys. J.* **536**, L63 (2000).
7. C. B. Netterfield *et al.*, in preparation (preprint available at xxx.lanl.gov/abs/astro-ph/0104460).
8. A. T. Lee *et al.*, preprint available at xxx.lanl.gov/abs/astro-ph/0104459.
9. C. J. Miller, D. J. Batuski, *Astrophys. J.*, in press.
10. C. J. Miller, K. S. Krughoff, D. J. Batuski, K. A. Slingsend, J. M. Hill, in preparation.
11. W. Saunders *et al.*, *Mon. Not. R. Astron. Soc.* **317**, 55 (2000).
12. A. J. S. Hamilton, M. Tegmark, in preparation (preprint available at xxx.lanl.gov/abs/astro-ph/0008392).
13. G. B. Dalton, G. Efstathiou, S. J. Maddox, W. J. Sutherland, *Mon. Not. R. Astron. Soc.* **271**, 47 (1994).
14. H. Tadros, G. Efstathiou, G. Dalton, *Mon. Not. R. Astron. Soc.* **296**, 995 (1998).
15. C. J. Miller, R. C. Nichol, D. J. Batuski, *Astrophys. J.*, in press.
16. We use the publicly available CMBFAST code to generate our cosmological models. This code is described by U. Seljak and M. Zaladarriga [*Astrophys. J.* **469**, 437 (1996)].
17. This is only true if we fix the Hubble constant, Ω_{matter} , and Ω_{vacuum} , thus altering only the curvature of the universe, which has no effect on the shape of the matter-density power spectrum.
18. S. Perlmutter *et al.*, *Astrophys. J.* **517**, 565 (1999).
19. A. G. Reiss, W. H. Press, R. P. Kirshner, *Astrophys. J.* **438L**, 17 (1995)

6 March 2001; accepted 14 May 2001
 Published online 24 May 2001;
 10.1126/science.1060440
 Include this information when citing this paper.

Conductance Switching in Single Molecules Through Conformational Changes

Z. J. Donhauser,¹ B. A. Mantooth,¹ K. F. Kelly,¹ L. A. Bumm,¹ J. D. Monnell,¹ J. J. Stapleton,¹ D. W. Price Jr.,² A. M. Rawlett,^{2*} D. L. Allara,^{1†} J. M. Tour,^{2†} P. S. Weiss^{1†}

We tracked over time the conductance switching of single and bundled phenylene ethynylene oligomers isolated in matrices of alkanethiolate monolayers. The persistence times for isolated and bundled molecules in either the ON or OFF switch state range from seconds to tens of hours. When the surrounding matrix is well ordered, the rate at which the inserted molecules switch is low. Conversely, when the surrounding matrix is poorly ordered, the inserted molecules switch more often. We conclude that the switching is a result of conformational changes in the molecules or bundles, rather than electrostatic effects of charge transfer.

Switches are among the most basic components for memory and logic, and some examples of molecules or nanostructures that might be used as switches have recently been demonstrated (1–11). We study such structures at the molecular scale to analyze and to understand mechanisms that cause conductance switching in single molecules. Stochastic switching of single-molecule fluorescence has been extensively studied spectroscopical-

ly (12, 13). We study another multistate phenomenon, conductance switching, with the scanning tunneling microscope (STM) in order to test which of the hypothesized mechanisms, if any, explain the switching.

Conjugated phenylene ethynylene oligomers have interesting and practical electronic characteristics in ensembles of thousands in nanopore experiments (6, 7, 11). Derivatives of these molecules have exhibited negative differential resistance (NDR) (increased resistance with increasing driving voltage), bistable conductance states (memory), and controlled switching under an applied electric field (6, 7, 11). Such characteristics are often attributed to charge transfer effects (14). Theoretical studies that have complemented the nanopore work suggest that the NDR and conductance switching of the molecules originate from an internal conformational twist that is induced by charge

¹Department of Chemistry, The Pennsylvania State University, University Park, PA 16802–6300, USA.

²Department of Chemistry and Center for Nanoscale Science and Technology, Rice University, Houston, TX 77005, USA.

*Present address: Motorola, 7700 South River Parkway, Tempe, AZ 85248, USA.

†To whom correspondence should be addressed. E-mail: dla3@psu.edu (D.L.A.); tour@rice.edu (J.M.T.); stm@psu.edu (P.S.W.)

transfer to the molecules (7, 14, 15). Low barriers to such internal rotations would make such states rather short-lived in comparison to measured persistence times reported in nanopores and in this work (11, 16).

In an effort to determine the important factors in the switching of these molecules on an individual basis, we studied this family of molecules using STM. Unlike the aforementioned nanopore experiments, the molecules are bound only to one gold electrode, and the STM tip acts as the second electrode that can individually address each molecule to determine its electronic and structural properties.

We have previously shown how two-dimensional matrix isolation of molecules in host self-assembled monolayers (SAMs) in combination with the STM and related methods can

be used to study the electronic properties of isolated and bundled molecules (17–20). In our earlier studies of matrix-isolated candidate molecular wires, exposure of the SAM to the molecular wires resulted in the molecules adsorbing at existing SAM defect sites and gold step edges with the long molecular axis aligned nearly normal to the gold surface (17–20). At these sites, the inserted molecules have access to the underlying gold substrate so that the sulfur head groups can chemisorb to the gold surface and the conjugated tails can protrude from the film. Because STM images are a convolution of the tip and surface structures, it is not always possible to distinguish individual from bundled molecules. For surface features with low corrugation, such as the molecular lattice of the matrix, STM images are good

representations of the surface structure. Details of features with higher aspect ratios, such as protruding molecules, can be more difficult to resolve with the STM and thus more difficult to interpret. As in our earlier work, we are able to infer that many of the like features at structural domain boundaries on substrate terraces, where access for insertion is limited, are individual molecules (18, 19).

Here, we used a dodecanethiolate monolayer matrix as a host to contain, support, and isolate phenylene ethynylene molecules. The rigid conjugated structures of the oligomers assure that conformational changes within the molecules are limited. We compared molecules that have demonstrated switching behavior in nanopore experiments, 2' and 3', with those that have not, 1' (Fig. 1). We found that all of these molecules switch conductance between two states. The switching has a strong correlation with the density of the surrounding matrix. We also demonstrated that the “switch” molecules, 2', can be deliberately switched from the ON to the OFF state using an applied electric field.

Typical dodecanethiolate matrix films (21) contain a variety of characteristic defect sites, including substrate step edges, film domain boundaries, and substrate vacancy islands (22). In Fig. 2A, several domain boundaries, a substrate vacancy island (in the lower right corner of the image), and one small bundle of 3' molecules (highlighted by the square) can be observed in the SAM. Series of images taken over time show the stability of the dodecanethiolate film. Well-ordered areas typically do not undergo substantial conformational changes, although some motion at domain boundaries can occasionally be observed. Because of the high packing density of the surrounding film, motion and conformational changes of the inserted molecules are partially hindered. In contrast to the stability of the host matrix, when individual or bundled molecules are observed over time, they frequently change conductance state or, depending on the type of defect, even move within the site. The inserted molecules have at least two states that differ in their apparent height in STM topography by ~ 3 Å. We refer to the more conductive state as “ON” (Fig. 2, A and B) and the less conductive state as “OFF” (Fig. 2, C and D).

The molecule in the OFF state still protrudes slightly from the host film, indicating that the inserted molecule is still present in the same defect site, a domain boundary in the matrix film. Because topographic STM images represent a convolution of the electronic and topographic structure of the surface, the apparent height change observed in the STM images can thus be due to a change in the physical height of the molecule, a change in the conductance of the molecule, or both. We observed this behavior for all three molecules studied, 1', 2', and 3'.

Switching between the ON and OFF states

Fig. 1. Molecules for which switching was observed (1', 2', and 3') are produced in situ from the corresponding thioacetlys (1, 2, and 3, respectively) with the deprotection reaction shown for each. Aqueous ammonium hydroxide is used to hydrolyze the acetyl protecting group, generating the thiolate or thiol. The thiolate/thiol can then adsorb on the Au{111} surface, inserting at existing defect sites in the dodecanethiolate monolayer matrix.

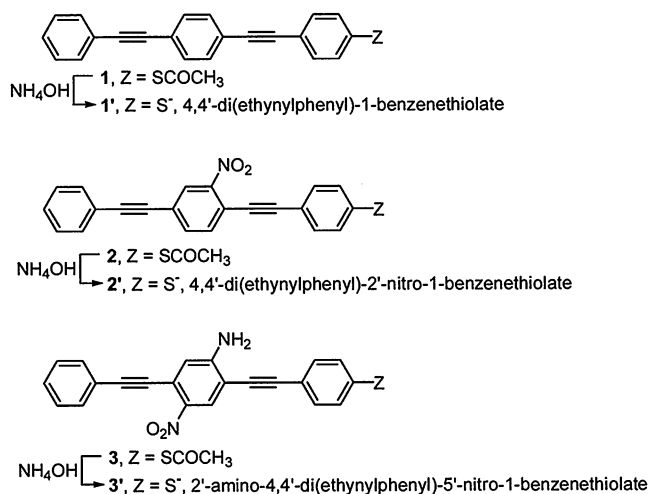
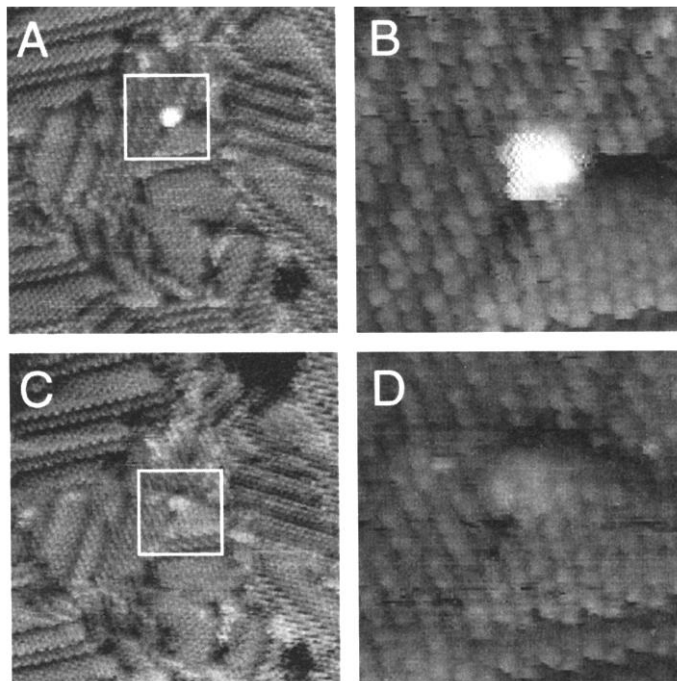


Fig. 2. Topographic STM images of a molecular switch, 3', inserted in a dodecanethiol SAM. The vertical scale on all images is ~ 8.5 Å. All images were acquired at a sample bias of -1.0 V and a current of 1.0 pA. (A) A 200 Å by 200 Å image of the molecule in the ON state and the surrounding SAM. A molecule of 3' is highlighted by the square. (B) A 50 Å by 50 Å image of the same area. The molecule is adsorbed in the domain boundary that separates the tightly packed dodecanethiol domains in the lower right and upper left areas of the image. (C) A 200 Å by 200 Å image of the same molecule in the OFF state. (D) A 50 Å by 50 Å image of the same area. The molecule in the OFF state still protrudes from the SAM.



REPORTS

was reversible (Fig. 3, A through C). A time-lapse series of images acquired over several (up to 26) hours recorded the long-time behavior of the molecules. Drift arising from thermal fluctuations and from creep in the STM piezoelectric imaging mechanism makes it difficult to observe a single small feature on the surface for long times; relatively large scan areas [(1000 to 2500 Å)²] were used to ensure that several molecules of interest remained in the area probed for the full duration of imaging. Additionally, large-scan areas allowed us to monitor several molecules simultaneously, enabling the statistical analysis of the switching. A tracking algorithm was developed to extract and to analyze small areas containing individual phenylene ethynylene molecules, **2'**, and then to measure their apparent height during the duration of the movie (23). Figure 3A is the large-scan area from which the data in Fig. 3, B and C, were extracted. In this case, several protrusions can be seen in the 1500 Å by 1500 Å image, showing several molecules of **2'** bound at a variety of defect sites and at gold substrate steps. Using our automated digital tracking and extraction algorithm, we monitored for the complete series of images the single molecule enclosed in the small square (Fig. 3A). The extracted images of this molecule are seen in the sequence shown in Fig. 3C. Reversible switching between the ON and OFF states occurs several times in the first 50 frames, recorded at 6-min intervals. The molecule then appears to stabilize in the ON state for the remainder of the images. From the extracted frames, the apparent topographic height versus the time was plotted for the selected molecule in Fig. 3B (24). In the OFF state, the molecule still appears to protrude slightly from the host film, indicating that it has remained bound to the same defect site. This reversible switching behavior was observed for **1'**, **2'**, and **3'**.

The insertion matrix plays a critical role in the switching of the guest molecules. By controlling the defect density and film quality, we changed the rates and numbers of molecules that switched. Two strategies were used to control the film quality. The first was to allow less time for self-assembly of the matrix so as to leave more and larger defect sites for insertion. Typical SAMs are made by exposing a gold surface to the alkanethiol solution for 24 hours. Although initial monolayer formation occurs rapidly, film restructuring and further ordering occurs for long times during exposure to the alkanethiol solution. To make SAMs with higher defect densities, we used a short (5 min) dodecanethiol deposition time. For this short deposition, the monolayer is essentially complete, but slower adsorption processes that increase order in the film have not yet completed. The result is a generally ordered film with high defect density.

A second strategy was used to improve film quality and reduce defect density. We annealed

the film in dodecanethiol vapor to add matrix molecules from the gas phase while avoiding exchange processes (which are inevitable during solution-phase annealing) (25). A SAM prepared over 24 hours and containing inserted **1'** was placed in a sealed vial containing a separate small amount of neat dodecanethiol. The contents were held at 80°C for 2 hours. The vapor-phase dodecanethiol molecules adsorbed at de-

fect sites, including around the guest molecules. It is assumed that desorption of the chemisorbed molecules from the film will be insignificant at 80°C. This procedure gives us a means to "backfill" around the inserted molecules without giving them a chance to desorb into solution. For **1'** inserted in the annealed film and **2'** inserted in the SAM prepared over 5 min, the effects of film processing were com-

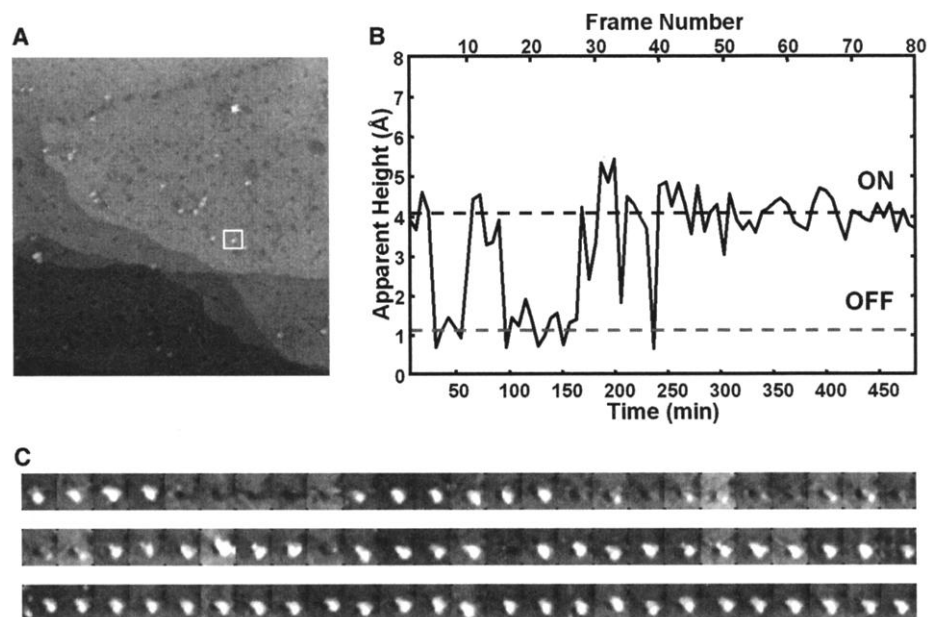
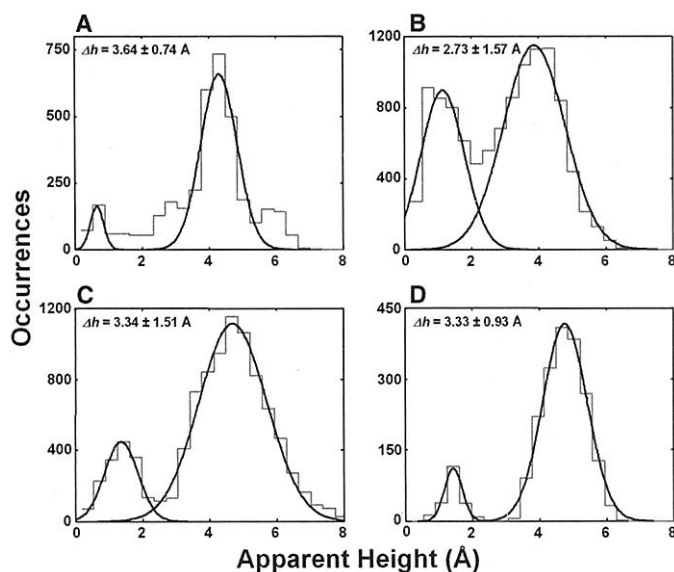


Fig. 3. (A) A 1500 Å by 1500 Å topographic STM image acquired at a sample bias of -1.4 V and a current of 0.2 pA. The vertical scale is ~ 30 Å. Several molecules of **2'** are inserted at the gold substrate step edges and the characteristic dodecanethiol SAM defect sites. The area in the small square is extracted from a sequential series of images to assemble the data in (B) and (C). (B) Height versus time for the molecule in the extracted area. Height is determined as described in (24). (C) Extracted frames of the selected molecule. The time interval between frames is ~ 6 min.

Fig. 4. Height distributions of **2'** [(A) and (B)] and **1'** [(C) and (D)]. All of the data were digitally extracted from series of images acquired over 20 hours at a sample bias of -1.0 V and a tunneling current of 1.0 pA. Heights are calculated as described in (24). Height distributions are given for molecules inserted in the following. (A) Dodecanethiol SAM prepared over 24 hours and then exposed to 0.1 μM **2'** for 0.5 hours. Gaussian best-fit parameters yield an OFF height (h_{off}) of 0.66 ± 0.20 Å and an ON height (h_{on}) of 4.30 ± 0.54 Å. (B) Dodecanethiol SAM prepared in 5 min and exposed to 0.1 μM **2'** for 0.5 hours ($h_{\text{off}} = 1.15 \pm 0.65$ Å; $h_{\text{on}} = 3.87 \pm 0.92$ Å). (C) Dodecanethiol SAM prepared over 24 hours and exposed to 0.1 μM **1'** for 0.5 hours ($h_{\text{off}} = 1.37 \pm 0.50$ Å; $h_{\text{on}} = 4.70 \pm 1.01$ Å). (D) Dodecanethiol SAM prepared over 24 hours, exposed to 0.1 μM **1'** for 0.5 hours, and then vapor annealed ($h_{\text{off}} = 1.43 \pm 0.27$ Å; $h_{\text{on}} = 4.76 \pm 0.66$ Å).



pared to the films produced from the standard 24-hour solution deposition. Other than the aforementioned processing steps, all of the samples were treated identically. The results of these experiments are summarized in Fig. 4 and Table 1.

Each histogram in Fig. 4 shows the distribution of heights for a representative sample of molecules extracted from a sequence of 200 images taken over 20 hours (Table 1). The apparent heights were calculated in the same fashion as for Fig. 3B. Bistability of the molecular conductances creates the prominent bimodal distribution; the peak at a lower apparent height results from molecules in the OFF state, whereas the other peak corresponds to the ON state. The distributions for **2'** in the (more ordered) SAM deposited for 24 hours and in the (more defective) SAM deposited for 5 min are shown in Fig. 4, A and B, respectively. Within experimental error, the apparent height difference between the ON and the OFF states is independent of matrix order, yet the average fraction of molecules in the OFF state increases dramatically in the "5-min" film. Fitting Gaussian distributions to each of the two peaks in Fig. 4A reveals the average apparent heights for the ON and OFF states, and the relative areas provide ON/OFF ratios of 12.3 for the more ordered SAM and 2.1 for the less ordered SAM matrices. This ratio reflects the lower observed switching activity in the more ordered films that could cause us to overlook switches that remain

OFF throughout the many hours of data acquisition. This problem arises because molecules continually in the OFF state are difficult to locate in large STM images and are thus less likely to be sampled; there are not necessarily fewer molecules in the OFF state. The greater conformational relaxation of host molecules in the more defective film allows the inserted molecules more freedom of movement. We conclude that the increased switching activity is caused by a conformational change of the inserted molecule. Additionally, the measured coverage of the inserted molecules in the less ordered film was found to be 2.6 times that of the more ordered film; these numbers are once again skewed by the undercount of molecules continuously OFF.

The effects of vapor annealing on switching were marked. The number of molecules observed in the OFF state decreased in the vapor-annealed film (Fig. 4D), as compared with the standard film (Fig. 4C). ON/OFF ratios were 5.2 for the unannealed film versus 9.2 for the vapor-annealed film. Thus, the host matrix can hinder switching when it is very well ordered, by obstructing conformational changes in the guest molecules (26).

Comparing the detailed results for **1'** and **2'** demonstrates that the molecules are qualitatively similar in their stochastic switching behavior. Switching of both is strongly correlated with host film order. Although the data presented in Table 1 may suggest that

the nitro functionalized molecule, **2'**, has greater switching activity, a full analysis of several data sets (not presented here) suggests that there is not a substantial difference between **1'** and **2'** in their stochastic switching activity. We conclude that the nitro functionality plays little role in the stochastic switching observed here and that the local environment is playing a much more critical role in mediating stochastic switching.

It is also important to examine the dependence of switching on electronic effects. To this end, we performed extensive studies in varying the tunneling current and the bias voltage. The magnitude of the tunneling current determines the number of electrons that are available to interact with local electronic states to induce such phenomena as local heating or electron attachment (27). The applied voltage creates large local electric fields that can interact with molecular or induced dipoles to drive molecular motion (28). We studied this system over a range of tunneling parameters: at bias voltages ranging from -1.4 to $+1.4$ V (with magnitudes as low as 500 mV) and at tunneling currents ranging from 0.1 to 4.0 pA. In this range of tunneling conditions, we observed no significant correlation with the amount of switching. From these experiments, we concluded that small differences in already low tunneling currents and voltages do not cause marked changes in the switching behavior and that more extreme tunneling conditions may be needed to effect switching.

At higher applied biases, we have had limited success in controllably switching the molecules from the ON to the OFF state. By applying voltages of magnitude greater than 3 V to the tip, we could switch molecules and bundles of **2'** into the OFF state (Fig. 5). In this case, four molecules of **2'** were switched OFF with a controlled pulse of 4.0 V to the tip (between Fig. 5, A and B). Figure 5C shows that at least one of the molecules has returned to the ON state after 74 min. These and similar experiments were successful both at high tunneling impedances ($>10^{12}$ ohms) and even when the tip was retracted 2 nm from this position. The resulting tip position is essentially out of tunneling range; thus, the magnitude of tunneling current is negligible. At these conditions, the effect on the tip-sample junction is therefore due to the applied electric field.

The higher voltages in the controlled switching experiments tend to degrade image quality (as in Fig. 5B), presumably because of structural changes in the matrix film, molecule, and/or tip. The controlled switching we observed is thus likely caused by conformational changes local to the molecule or bundle of interest. Our attempts to switch molecules from OFF to ON have been less successful and may require higher applied voltages.

Host films and individual sites with higher degrees of conformational relaxation allow

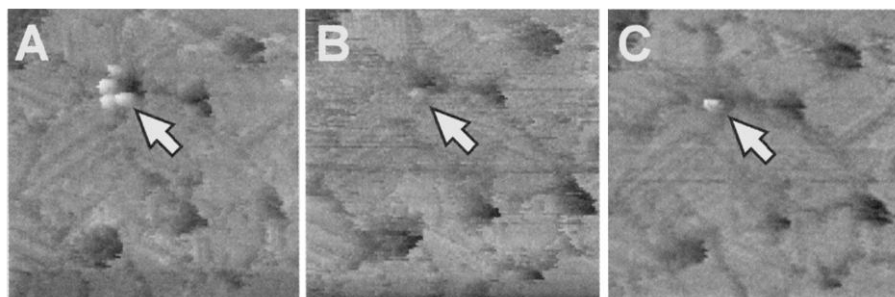


Fig. 5. Images of four molecules of **2'** (indicated by arrows) in a dodecanethiolate film. All images are 1000 Å by 1000 Å and were acquired at +1.0 V sample bias and 0.7 pA. The vertical scale is ~ 10 Å for all images. (A) The initial state of the molecules is ON. (B) Immediately before this image, the tip was retracted 2 nm from its imaging position at 1.4×10^{12} ohms, and the voltage was ramped up to +4 V. Upon imaging, the molecules appear in the OFF state. (C) After 74 min, at least one of the molecules returned to the ON state.

Table 1. Summary of data for bimodal distributions that were obtained from four different dodecanethiol SAMs (Fig. 4). The percentage that switched was calculated on the basis of all sampled molecules, including those that may have drifted out of the field of view during data acquisition. This may slightly lower the calculated percentage that switched, because an inactive molecule may undergo a switching event after leaving the field of view.

Matrix preparation	Insertion coverage (molecules/Å ²)	Inserted molecule	Number sampled	Percentage that switched	ON/OFF ratio
5 min	32.9×10^{-6}	2'	74	47	2.1
24 hours	12.4×10^{-6}	2'	28	32	12.3
24 hours	25.3×10^{-6}	1'	57	11	5.2
24 hours*	6.7×10^{-6}	1'	15	7	9.2

*Vapor annealed

more freedom of movement for the guest molecules, leading to higher switching rates. Indeed, the persistence times measured for the switches in (11) may provide a measure of the order within the nanopore. Molecules that switch remain bound to the same location on the substrate. This group of phenylene ethynylene oligomers, 1', 2', and 3', is qualitatively similar in that they exhibit bistable conductance when inserted into dodecanethiol films; the nitro substituent is not the determining factor in the stochastic conductance switching observed here. We also demonstrated the ability to induce switching, using high electric fields to control the conductance states in 2'.

References and Notes

- J. M. Tour, M. Kozaki, J. M. Seminario, *J. Am. Chem. Soc.* **120**, 8486 (1998).
- J. M. Tour, *Acc. Chem. Res.* **33**, 791 (2000).
- S. J. Tans, A. R. M. Vershueren, C. Dekker, *Nature* **393**, 49 (1998).
- C. P. Collier et al., *Science* **285**, 391 (1999).
- C. P. Collier et al., *Science* **289**, 1172 (2000).
- J. Chen, M. A. Reed, A. M. Rawlett, J. M. Tour, *Science* **286**, 1550 (1999).
- J. Chen et al., *Appl. Phys. Lett.* **77**, 1224 (2000).
- C. Joachim, J. K. Gimzewski, R. R. Schlittler, C. Chavy, *Phys. Rev. Lett.* **74**, 2102 (1995).
- F. Moresco et al., *Phys. Rev. Lett.* **86**, 672 (2001).
- D. I. Gittins, D. Bethell, D. J. Schiffrin, R. J. Nichols, *Nature* **408**, 67 (2000).
- M. A. Reed et al., *Appl. Phys. Lett.* **78**, 3735 (2001).
- W. E. Moerner, M. Orrit, *Science* **283**, 1670 (1999).
- X. S. Xie, *Acc. Chem. Res.* **29**, 598 (1996).
- J. M. Seminario, A. G. Zacarias, J. M. Tour, *J. Am. Chem. Soc.* **122**, 3015 (2000).
- M. D. Ventra, S. T. Pantelides, N. D. Lang, *Phys. Rev. Lett.* **84**, 979 (2000).
- J. M. Seminario, A. G. Zacarias, J. M. Tour, *J. Am. Chem. Soc.* **120**, 3970 (1998).
- P. S. Weiss et al., *Ann. N.Y. Acad. Sci.* **852**, 145 (1998).
- M. T. Cygan et al., *J. Am. Chem. Soc.* **120**, 2721 (1998).
- L. A. Bumm et al., *Science* **271**, 1705 (1996).
- T. D. Dunbar et al., *J. Phys. Chem. B* **104**, 4880 (2000).
- The SAM matrices were prepared on commercial Au(111) on mica (Molecular Imaging, Phoenix, AZ). The gold substrates were annealed and cleaned with a hydrogen flame immediately before film preparation. SAM matrices were deposited from a 1 mM solution of dodecanethiol in ethanol. The samples were then rinsed in neat ethanol and blown dry with nitrogen. Solutions were prepared that were 0.1 mM of 1, 2, or 3 in dry tetrahydrofuran. Aqueous ammonia was added to hydrolyze the acetyl protecting group, generating the thiol in situ to adsorb as the thiolate (1', 2', or 3') on the surface. The exposure time of the host matrix to the guest molecules typically ranged from several minutes to a few hours. After rinsing and drying, the samples were stored at room temperature in a desiccator. STM imaging was performed under ambient conditions as previously described (18, 19).
- G. E. Poirier, *Chem. Rev.* **97**, 1117 (1997).
- Movies are available as supplementary material at <http://stm1.chem.psu.edu/supplemental/switch.html>.
- Each frame was median filtered. The topographic height was then assigned as the median of the highest nine points in the frame minus the median of the lowest fourth of the extracted image. Thus, an apparent height of 0 would only occur if the image was almost perfectly flat. The extracted frames shown in Fig. 3 were interpolated to twice the pixel density and median filtered.
- G. E. Poirier, E. D. Pylant, *Science* **272**, 1145 (1996).
- The annealing process decreases the number of inserted molecules observed in the film. We cannot yet

- attribute this change to desorption from the film or degradation of the molecules at elevated temperatures.
- C. F. Herrmann, J. J. Boland, *J. Phys. Chem. B* **103**, 4207 (1999).
 - H. C. Akpati, P. Norlander, L. Lou, P. Avouris, *Surf. Sci.* **372**, 9 (1997).
 - We thank A. Hatzor, P. Lewis, G. McCarty, and R.

Smith for experimental assistance and M. Ratner for helpful discussions. The continuing support of the Army Research Office, the Defense Advanced Research Projects Agency, the NSF, the Office of Naval Research, and Zyvex are most gratefully acknowledged.

28 February 2001; accepted 9 May 2001

A 14,000-Year Oxygen Isotope Record from Diatom Silica in Two Alpine Lakes on Mt. Kenya

P. A. Barker,¹ F. A. Street-Perrott,² M. J. Leng,³ P. B. Greenwood,³ D. L. Swain,^{2*} R. A. Perrott,² R. J. Telford,^{1†} K. J. Ficken²

Oxygen isotopes are sensitive tracers of climate change in tropical regions. Abrupt shifts of up to 18 per mil in the oxygen isotope ratio of diatom silica have been found in a 14,000-year record from two alpine lakes on Mt. Kenya. Interpretation of tropical-montane isotope records is controversial, especially concerning the relative roles of precipitation and temperature. Here, we argue that Holocene variations in $\delta^{18}\text{O}$ are better explained by lake moisture balance than by temperature-induced fractionation. Episodes of heavy convective precipitation dated ~11,100 to 8600, 6700 to 5600, 2900 to 1900, and <1300 years before the present were linked to enhanced soil erosion, neoglacial ice advances, and forest expansion on Mt. Kenya.

Paleoclimate records from tropical regions are essential to understanding past changes in Earth's climate system, equator-pole linkages (1), and the sensitivity of tropical regions to future climate change (2). High-resolution oxygen isotope records from Andean ice cores reveal the response of tropical mountain climates to global forcing during the Last Glacial Stage and Holocene (2). On Mt. Kenya, however, ice-core studies of the rapidly retreating mountain glaciers have proved unsuccessful because of meltwater percolation (3, 4). As an alternative, ^{18}O measurements can be made on diatom silica ($\delta^{18}\text{O}_{\text{diatom}}$) from the sediments of high-altitude lakes. A 3000-year $\delta^{18}\text{O}_{\text{diatom}}$ record obtained from Hausberg Tarn [4370 m above sea level (asl)], a glacier-fed lake on the northwest flank of Mt. Kenya (5), contained short-term minima in $\delta^{18}\text{O}_{\text{diatom}}$ attributed to glacier melting and longer term minima attributed to increased water temperatures (5, 6), in contrast to the pos-

itive relation assumed between $\delta^{18}\text{O}$ and air temperature in ice-core studies (7). Here, we present a 14,000-year $\delta^{18}\text{O}_{\text{diatom}}$ record compiled from two adjacent but hydrologically independent tarns located on the climatically sensitive northeast flank of Mt. Kenya. Their catchments have not been glaciated during the last 14,000 years (6).

Small Hall Tarn (SHT; 0°9'S, 37°21'E, 4289 m asl) is a topographically closed lake (0.5 m deep in January 1996) in the Gorges Valley. Simba Tarn (ST; 0°9'S, 37°19'E, 4595 m asl) is an open lake near the head of the Gorges Valley; in January 1996 it had a maximum depth of 5 m and an electrical conductance of just 18.9 $\mu\text{S cm}^{-1}$. Precipitation in the summit zone of Mt. Kenya falls mainly from March to May and in October and November, although some occurs in every month. Total precipitation declines with altitude above the tree line (~3000 m asl) and is <900 mm a^{-1} above 4500 m asl, where it mainly falls as snow (3). The main moisture source is the southwest Indian Ocean, because of southeasterly airflow in the lower troposphere during the rainy seasons (3, 8). Mean annual temperatures are close to freezing at both sites (+1.3°C at SHT, -0.7°C at ST), with a monthly variability of $\pm 2^\circ\text{C}$ but a large diurnal range (10° to 20°C) (3). Terrestrial plant cover is moderate (SHT) to very sparse (ST) at present.

Piston cores raised in 1996 from SHT and ST were dated by accelerator mass spectrometry, yielding 12 ^{14}C dates for SHT and 10 ^{14}C dates for ST (9). They were analyzed

¹Hysed, Department of Geography, Lancaster University, Lancaster LA1 4YB, UK. ²Tropical Palaeoenvironments Research Group, Department of Geography, University of Wales Swansea, Swansea SA2 8PP, UK. ³Natural Environment Research Council (NERC) Isotope Geoscience Laboratory, Keyworth, Nottingham NG12 5GG, UK.

*Present address: Scottish Agricultural College, Crichton Royal Farm, Dumfries DG1 4SZ, UK.

†Present address: Department of Geography, University of Newcastle, Newcastle-upon-Tyne NE1 7RU, UK.